

## Phase Behavior of Stratum Corneum Lipids in Mixed Langmuir–Blodgett Monolayers

E. ten Grotenhuis,\* R. A. Demel,# M. Ponec,§ D. R. Boer,\*\* J. C. van Miltenburg,\* and J. A. Bouwstra<sup>¶</sup>

\*Debye Institute, Department of Interfaces and Thermodynamics, Utrecht University, Utrecht, The Netherlands; #Center for Biomembranes and Lipid Enzymology, Department of Biochemistry of Membranes, Utrecht University, Utrecht, The Netherlands;

§University Hospital, Department of Dermatology, Leiden, The Netherlands; ¶Leiden/Amsterdam Center for Drug Research, Gorlaeus Laboratories, Leiden University, Leiden, The Netherlands

**ABSTRACT** The lipids found in the bilayers of the stratum corneum fulfill the vital barrier role of mammalian bodies. The main classes of lipids found in stratum corneum are ceramides, cholesterol, and free fatty acids. For an investigation of their phase behavior, mixed Langmuir–Blodgett monolayers of these lipids were prepared. Atomic force microscopy was used to investigate the structure of the monolayers as a function of the monolayer composition. Three different types of ceramide were used: ceramide extracted from pigskin, a commercially available ceramide with several fatty acid chain lengths, and two synthetic ceramides that have only one fatty acid chain length. In pigskin ceramide–cholesterol mixed monolayers phase separation was observed. This phase separation was also found for the commercially available type III Sigma ceramide–cholesterol mixed monolayers with molar ratios ranging from 1:0.1 to 1:1. These monolayers separated into two phases, one composed of the long fatty acid chain fraction of Sigma ceramide III and the other of the short fatty acid chain fraction of Sigma ceramide III mixed with cholesterol. Mixtures with a higher cholesterol content consisted of only one phase. These observations were confirmed by the results obtained with synthetic ceramides, which have only one fatty acid chain length. The synthetic ceramide with a palmitic acid (16:0) chain mixed with cholesterol, and the synthetic ceramide with a lignoceric acid (24:0) chain did not. Free fatty acids showed a preference to mix with one of these phases, depending on their fatty acid chain lengths. The results of this investigation suggest that the model system used in this study is in good agreement with those of other studies concerning the phase behavior of the stratum corneum lipids. By varying the composition of the monolayers one can study the role of each lipid class in detail.

### INTRODUCTION

The skin protects the mammalian body against harmful influences from outside and permits control of the internal environment. The barrier function of the skin is fulfilled by the outermost layer of the epidermis, the stratum corneum (SC). The SC consists of dead, flattened cells, the keratin-filled corneocytes, embedded in lipid lamellar regions. These lamellae are very rigid. The lamellae are composed of ceramides, cholesterol, and free fatty acids (Wertz and Downing, 1991; Schurer and Elias, 1991). In the SC a series of ceramides is present (Wertz and Downing, 1983). Ceramides consist of a sphingosine or a phytosphingosine as the long-chain base with nonhydroxy or  $\alpha$ -hydroxy fatty acid in amide linkage. The differences among the seven classes of ceramides present in pig epidermis are summarized in Table 1.

It was shown that the vital barrier function of the SC is almost entirely attributable to the intercellular lipid regions (Elias, 1983). The presence of intercellular lamellae was first visualized by freeze fracture electron microscopy (Breathnach et al., 1973). Small-angle x-ray diffraction experiments on human, pig, and mouse SC confirmed that the

lipids are arranged as lamellar, possibly bilayer, structures. In mouse SC White et al. (1988) found one repeat distance, which had a periodicity of 13.1 nm. Bouwstra et al. (1994) occasionally found a second lipid lamellar phase with a periodicity of 6.1 nm. Small-angle x-ray diffraction measurements of porcine SC also indicate the presence of two phases, one with a spacing of 6.0 nm and the other with a spacing of 13.2 nm (Bouwstra et al., 1995). In human SC the repeat distances of the lamellar phases were found to be 6.4 and 13.4 nm (Bouwstra et al., 1991).

Studies have been carried out to attempt reproduction of the lipid organization of intact SC (Parrott and Turner, 1993) by preparing a model system from a mixture of cholesterol and Sigma ceramide III, which belongs to the ceramide 2 family. Parrott and Turner performed small-angle x-ray diffraction measurements of their model system. They showed that two lipid phases were present, one with a periodicity of 10.4 nm and a second with a periodicity that decreased from 5.5 nm for pure ceramide to 4.5 nm for a ceramide–cholesterol mixture with a molar ratio of 1:1. At higher cholesterol concentrations the 10.4-nm periodicity did not occur. The two-phase system corresponded well to the two-phase organization of intact SC. Parrott and Turner suggested that the long repeat distance phase is a mixture of ceramide and cholesterol with a fixed composition. In a more recent study a similar model system was prepared from a hydrated mixture at pH 5.0 (similar to the pH in intact SC) of ceramides extracted from pigskin and commercially available cholesterol (Bouwstra et al., 1996). It

Received for publication 22 January 1996 and in final form 4 June 1996.

Address reprint requests to Dr. Erik ten Grotenhuis, Department of Interfaces and Thermodynamics, Debye Institute, Utrecht University, Padualaan 8, 3584 CH Utrecht, The Netherlands. Tel.: 31-30-2533211; Fax: 31-30-2533946; E-mail: grotenh@chem.ruu.nl.

© 1996 by the Biophysical Society

0006-3495/96/09/1389/11 \$2.00

**TABLE 1** Compositional data for pig epidermal ceramides

Ceramide	Long-Chain Base	Amide-Linked Fatty Acid	Esterified Fatty Acid	Number of Free Hydroxyls
1	Sphingosine	$\omega$ -OH	Nonhydroxy	2
2	Sphingosine	Nonhydroxy	None	2
3	Phytosphingosine	Nonhydroxy	None	3
4	Sphingosine	$\alpha$ -OH (C <sub>24</sub> -C <sub>28</sub> )	None	3
5	Sphingosine	$\alpha$ -OH (C <sub>16</sub> )	None	3
6a	Sphingosine	$\omega$ -OH	$\alpha$ -OH	3
6b	Phytosphingosine	$\alpha$ -OH	None	4

was shown that the phase behavior of isolated ceramides mixed with cholesterol in a wide range of molar ratios was similar to that of intact SC. Two lamellar phases were found, with spacings of 5.2 and 12.2 nm. It was also shown that the addition of free fatty acids increases the solubilization of cholesterol in the lamellar phases. This and other studies suggest that for the formation of the characteristic lamellar structures in the intercorneocyte space the presence of ceramides and cholesterol is a prerequisite.

Despite the information obtained from these experiments, there is still some ambiguity about the composition of each of the phases present in the SC. The aforementioned studies all used techniques that give information averaged over a relatively large volume of the samples studied, and a more detailed study is necessary to elucidate the phase behavior of mixtures of SC lipids.

To investigate further the phase behavior of SC lipids one can apply atomic force microscopy (AFM) to obtain higher lateral resolution. Samples suitable for AFM characterization have to be prepared in a well-defined manner. The Langmuir-Blodgett technique has proved to be a suitable method to prepare monolayers of amphiphilic molecules. Löfgren and Pascher (1977) used the Langmuir technique to study the area per molecule and the compressibility of a series of synthetic ceramides. At low surface pressures they found that the conformation of the molecules was determined mainly by the interaction between the polar headgroups of the ceramides and the water surface. At 30 mN/m, a lateral pressure corresponding to that of biological membranes, the molecular areas also depended on the arrangement of the hydrophobic chains.

The Langmuir-Blodgett technique can be used to prepare mixed monolayers of amphiphilic molecules on solid substrates. AFM and friction force microscopy have been used to study mixed monolayers of arachidic acid and partially fluorinated carboxylic ether acid (Meyer et al., 1992; Overney et al., 1992, 1994; Fujihara and Tanako, 1994), mixed monolayers of 5,10,15-triphenyl-20-(4-DL-phenylalanylaminido)phenylporphyrin and arachidic acid (Wu et al., 1995), stearic acid (Xiao et al., 1995) or L- $\alpha$ -dipalmitoylphosphocholine (Yang et al., 1994), and mixed monolayers of octadecyltrichlorosilane and 2-(perfluorooctyl)trichlorosilane (Ge et al., 1995). These studies have shown that it is possible to detect separate phases of different types of molecule within a monolayer. The majority of these AFM

images show that circular domains representing a phase rich in one type of molecule were formed in a matrix that was rich in the other type of molecule. In some cases domain nets were formed (Xiao et al., 1995). Besides the shape of the domains, the size and the difference in height between different domains can also be determined with AFM. The latter information is important in determining whether molecules are arranged as monolayers or that one type of molecule is pushed out of the monolayer and is deposited on top of the other type of molecule.

The aim of our study is to use AFM to investigate the phase behavior of mixtures of SC lipids in a monolayer prepared with the Langmuir-Blodgett technique. Applying AFM to elucidate the phase behavior of SC lipids may provide insight into the role of ceramides and cholesterol in the permeability barrier function of the SC.

## MATERIALS AND METHODS

### Materials

Bovine brain ceramide type III ( $\Sigma$ CerIII) was obtained from Sigma Chemical Co. (St. Louis, MO).  $\Sigma$ CerIII contains primarily stearic (18:0) and nervonic (24:1) amide-linked fatty acids. The headgroup of  $\Sigma$ CerIII is a sphingosine group, similar to that of ceramide 2 present in large quantities in SC. Two synthetic ceramides, one composed of palmitic (16:0; PA) and one of lignoceric (24:0; LA) acid amide-linked to a phytosphingosine base, were prepared by Gist Brocades, Cosmoferm b.v. (Delft, the Netherlands), and made available by Beiersdorf AG (Hamburg, Germany). These will be referred to as C16cer3 and C24cer3, respectively. Pigskin ceramides were isolated from fresh skin following the procedure described by Bouwstra et al. (1996). This ceramide, referred to as Tcer in this paper, contains nonhydroxy and  $\alpha$ -hydroxy fatty acids amide linked to (phyto)sphingosine bases. Cholesterol (Chol; cholest-5-en-3 $\beta$ -ol) was purchased from Merck (Darmstadt, Germany). Free fatty acids were obtained from Sigma.

### Preparation of monolayers

Silicon wafers were used as supports for the Langmuir-Blodgett films. The wafers were cut into strips (10 mm  $\times$  40 mm) suitable for monolayer transfer. We made the surfaces of the silicon strips hydrophilic before transfer of the monolayers by cleaning the wafers with a boiling H<sub>2</sub>O<sub>2</sub>/NH<sub>4</sub>OH/H<sub>2</sub>O (1:1:5 v/v) mixture and rinsing with distilled water. Ceramides and mixtures of ceramides with cholesterol, free fatty acids, or both were dissolved in chloroform-methanol (5:1 v/v) and spread on the air-water surface. We compressed the monolayer films to a pressure of 30 mN/m and transferred them to the hydrophilic silicon surfaces by vertically lifting the supports with a speed of 3 mm/min through the air-water interface at constant surface pressure, forming Z-type Langmuir-Blodgett

films. Each lipid mixture was prepared and subsequently transferred at least three times.

## AFM measurements

The samples were examined with an AFM within 6 h after preparation. Different areas of each sample were examined to ensure that the samples were homogeneous. Measurements were performed with a Nanoscope III microscope (Digital Instruments Inc.) under atmospheric conditions. Microfabricated cantilevers (length 100  $\mu\text{m}$ , spring constant 0.6  $\text{N m}^{-1}$ ) with an integrated pyramidal tip were used. All images were acquired without filtering in constant force mode, i.e., the distance between the tip and the sample was kept constant. The samples were mounted on a D-type piezo tube, which had a scan range of 14 ( $x$ )  $\mu\text{m} \times 14$  ( $y$ )  $\mu\text{m} \times 4$  ( $z$ )  $\mu\text{m}$ . The deflection of the cantilever was monitored by the reflection of a laser beam from the back of the cantilever onto a horizontally split detector.

## RESULTS

### Chain length of fatty acids in ceramides

In pigskin several types of ceramide are present. Table 2 shows the distribution of the ceramides present in pigskin SC. The ceramide types are numbered according to Wertz et al. (1993). The chain-length distribution of the amide linked fatty acids is listed in Table 3. A bimodal distribution was found. The fatty acid chain length distribution of  $\Sigma\text{CerIII}$  is also given in Table 3.

### Surface-pressure area isotherms

The surface-pressure ( $\Pi$ ) area ( $A$ ) isotherms were recorded for pure cholesterol and for the ceramides used in this study (Fig. 1). At a surface pressure of 30  $\text{mN/m}$ , the pressure at which the monolayers were transferred to the silicon substrate, we found for cholesterol a surface area per molecule of 40  $\text{\AA}^2$ . For the ceramides the molecular surface area at 30  $\text{mN/m}$  ranged from 40  $\text{\AA}^2$  for C16cer3 to 50  $\text{\AA}^2$  for  $\Sigma\text{CerIII}$ . Mixing ceramides with cholesterol did not result in a deviation from the additivity rule. This means that the mean molecular areas of the mixed films of two components follow the additivity rule:  $A(\pi) = x_1 A_1(\pi) + (1 - x_1) A_2(\pi)$ , where  $A_1$  and  $A_2$  are the areas per molecule in pure monolayers of components 1 and 2, respectively, and  $x_1$  is the mole fraction of component 1. This does not imply that the mixtures were ideal. A deviation from the additivity rule is proof of phase separation, but phase separation does not necessarily lead to a deviation from the additivity rule.

**TABLE 2** Ceramide profile in pig stratum corneum

Ceramide	w/w %
1	7.8
2	55.4
3	17.6
4	3.6
5	9.9
6a	5.6

**TABLE 3** Chain distribution of nonhydroxy and  $\alpha$ -hydroxy amide linked fatty acids in pigskin ceramide and in  $\Sigma\text{CerIII}$

Alkyl Chain	Pigskin Ceramides		$\Sigma\text{CerIII}$ Nonhydroxy Fatty Acids
	Nonhydroxy Fatty Acids	$\alpha$ -Hydroxy Fatty Acids	
14:0		2.6	
16:0	3.1	45.7	1.7
18:0	3.0		31.6
18:1	2.8		
18:2	5.7		
20:0	12.0	11.5	
22:0	11.5	6.3	2.9
22:1			1.3
22:3			2.1
22:4			1.5
24:0	25.8	27.7	6.9
24:1			47.9
25:0	2.8		1.5
26:0	12.6	2.1	
28:0	10.4		

The percentages are given in % w/w.

### Pigskin ceramide–cholesterol mixtures

The interfacial mobility of the platinum plate used to measure the surface pressure indicated that pure TCer Langmuir monolayers were very rigid. An AFM image of a transferred TCer monolayer is shown in Fig. 2 A. The monolayer has an irregular surface with many small holes and ripples. Adding cholesterol to TCer had a fluidizing effect on the monolayer. In the AFM image shown in Fig. 2 B two phases can be observed in a monolayer prepared with a TCer–Chol molar ratio of 1:0.2. Small domains, which appear as bright regions in the AFM image, are present in the monolayer. The domains are  $8 \pm 1$   $\text{\AA}$  thicker than the rest of the monolayer. Increasing the cholesterol content to a 1:1 molar ratio results in a similar monolayer structure, which also reveals two phases (Fig. 2 C). The AFM image of monolayer prepared with a TCer–Chol mixture with a ratio of 1:2 also showed two separate phases (Fig. 2 D). Hence, for all TCer–Chol ratios used to prepare monolayers, two clearly separated phases were found.

### Sigma ceramide III–cholesterol mixtures

Pure sigma ceramide III ( $\Sigma\text{CerIII}$ ) Langmuir monolayers were very rigid. This was reflected in the AFM image of the transferred monolayer of pure  $\Sigma\text{CerIII}$  (Fig. 3 A). The monolayer has a rippled surface with a substantial number of small defects. The defects are too small to determine the thickness of the film with the AFM, because the tip does not reach the substrate.  $\Sigma\text{CerIII}$ –Chol mixtures were prepared with an increasing fraction of cholesterol. These mixtures were also spread on the air–water interface. The increased mobility of the platinum plate indicated that the monolayer became more fluid when we added more cholesterol. An AFM image of a monolayer prepared with a  $\Sigma\text{CerIII}$ –Chol molar ratio of 1:0.1 is shown in Fig. 3 B. Already at this relatively low cholesterol concentration we did not observe

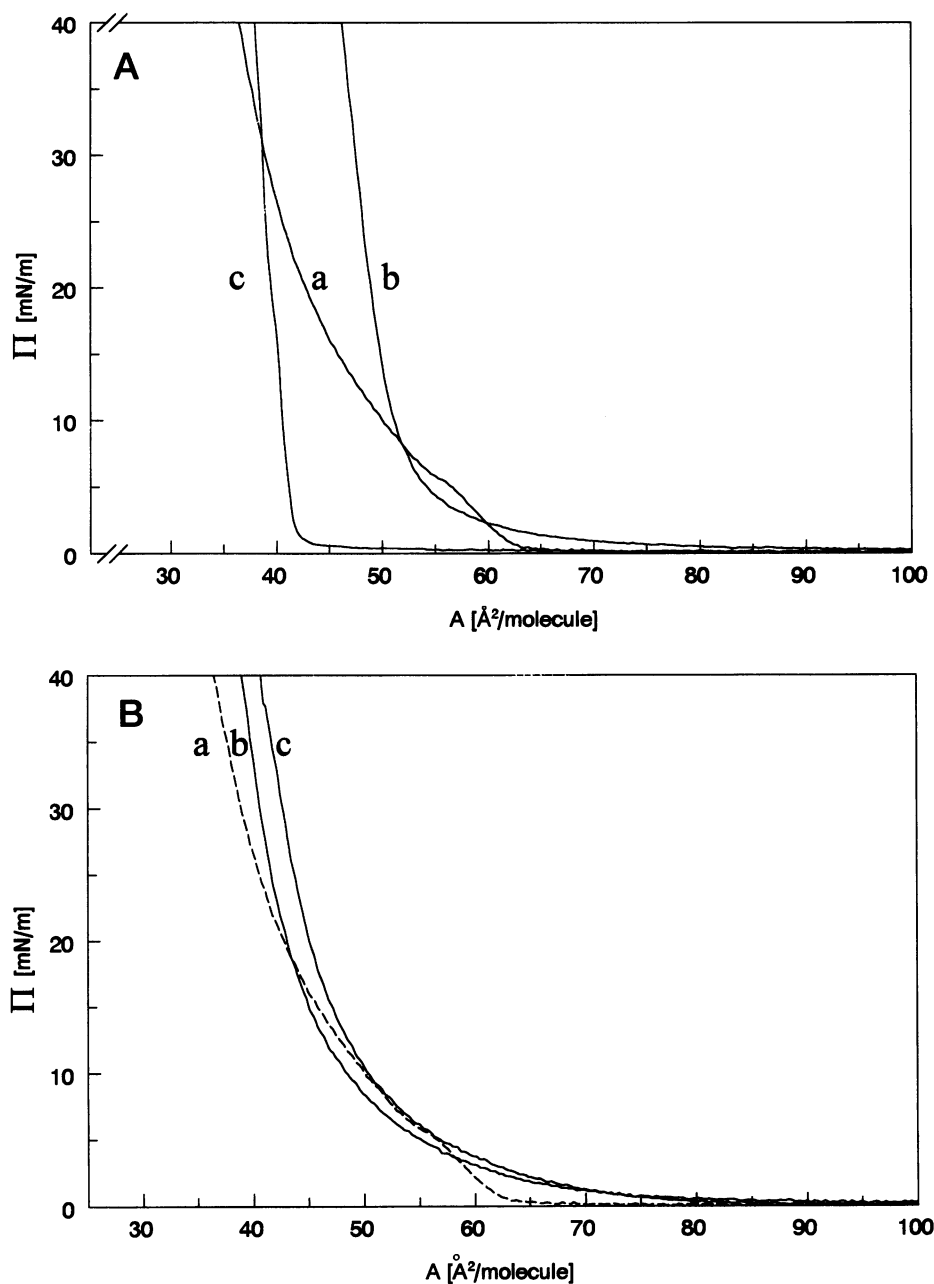


FIGURE 1 (A)  $\Pi$  A isotherms of (a) pigskin ceramide, (b)  $\Sigma$ CerIII, and (c) cholesterol. (B)  $\Pi$  A isotherms of (a) pigskin ceramide, (b) C16cer3, and (c) C24cer3.

any defects in the monolayer, and the ripples were also absent. Fig. 3 B shows a monolayer that consists of two phases that have a difference in monolayer thickness of  $5 \pm 1$  Å. A large part of the surface (90%) is covered with domains of a higher phase, A, which appear as lighter-colored areas in the AFM image. The remaining 10% of the surface is covered by a lower, darker-colored phase, B. Gradually increasing the cholesterol content of the monolayer from 1:0.1 to 1:1, we observed with the AFM that the fraction of the surface covered with phase A decreased while, obviously, the fraction covered by phase B increased (Fig. 3 C–E). At a  $\Sigma$ CerIII–Chol molar ratio of 1:0.6 (Fig. 3 D) the domains of phase A are still connected with each other. At higher cholesterol concentrations phase A exists as separate domains in the phase B matrix. The shapes of the

domains are not round but resemble flow patterns in a liquidlike film. The difference in monolayer thickness between phases A and B was  $5 \pm 1$  Å for the AFM images shown in Fig. 3 B–E. At cholesterol concentrations higher than 1:1 the domains were not observed. Fig. 3 F is an AFM image of a monolayer prepared with a 1:2  $\Sigma$ CerIII–Chol mixture. The relatively homogeneous monolayer showed no significant height variations.

#### Mixed monolayers involving C16cer3, C24cer3, and cholesterol

To obtain support for a preferential mixing of cholesterol with the short- or long-chain species of  $\Sigma$ CerIII, we studied

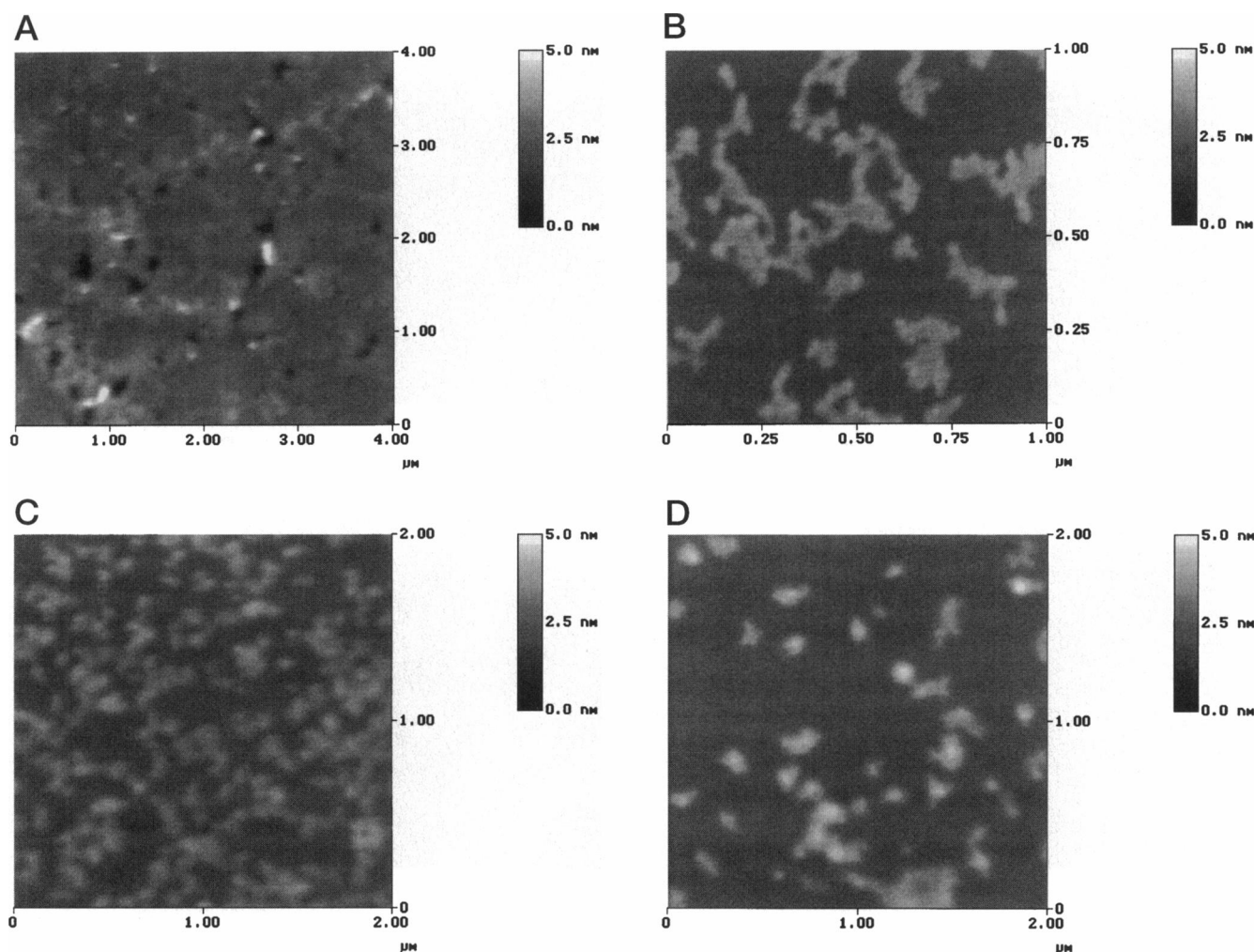


FIGURE 2 AFM images of areas of pigskin ceramide–cholesterol mixed monolayers deposited upon silicon oxide substrates. The ratios are (a) 1:0, (b) 1:0.2, (c) 1:1, and (d) 1:2. Note that these images do not have the same lateral dimensions.

synthetic ceramides with defined fatty acid chain lengths. Monolayers prepared from pure synthetic ceramides were very rigid, just like  $\Sigma$ CerIII monolayers. An AFM image of a C24cer3 Langmuir–Blodgett monolayer is shown in Fig. 4 A. The monolayer showed a relatively large number of small defects and revealed a rough surface. C16cer3 monolayers had a similar structure (results not shown). Mixing cholesterol with these ceramides caused a much more fluidlike character of the monolayers at the air–water interface. Fig. 4 B shows an AFM image of a transferred mixed monolayer prepared from C16cer3 and cholesterol in an equimolar ratio. No phase separation was observed, and the height of the film was very homogeneous. The longer C24cer3 molecules demonstrated a totally different phase behavior when they were mixed with cholesterol. The AFM image (Fig. 4 C) of a transferred monolayer prepared with a 1:1 C24cer3–Chol mixture revealed a film with small, interconnected domains. The difference in monolayer thickness between the domains and the surrounding molecules was  $6 \pm 1 \text{ \AA}$ . We used the synthetic ceramides to try to

simulate the phase behavior of  $\Sigma$ CerIII. Inasmuch as  $\Sigma$ CerIII itself is a mixture of ceramides with mainly 18:0 and 24:1 fatty acid chains, we mixed C16cer3 and C24cer3 at a molar ratio of 1:1 to obtain a similar chain-length distribution. C16cer3 was used instead of a synthetic ceramide with an amide-linked 18:0 fatty acid because it has approximately the same length as the cholesterol molecule. An AFM image of a monolayer prepared with the C16cer3:C24cer3 mixture without the addition of cholesterol is shown in Fig. 4 D. The defects in this monolayer were very small. The structure was similar to that of pure C24cer3. No phase separation was observed in this monolayer. Finally, we added cholesterol to the C16cer3–C24cer3 mixture in a molar ratio of 1:1:2 (C16cer3:C24cer3:Chol). Fig. 4 E shows an AFM image of a transferred monolayer of this mixture. Domains were observed in this film. However, these domains were not distributed homogeneously in the monolayer. The shapes of the domains was similar to the shapes of the domains found in a 1:1 C24cer3–Chol mixed monolayer.

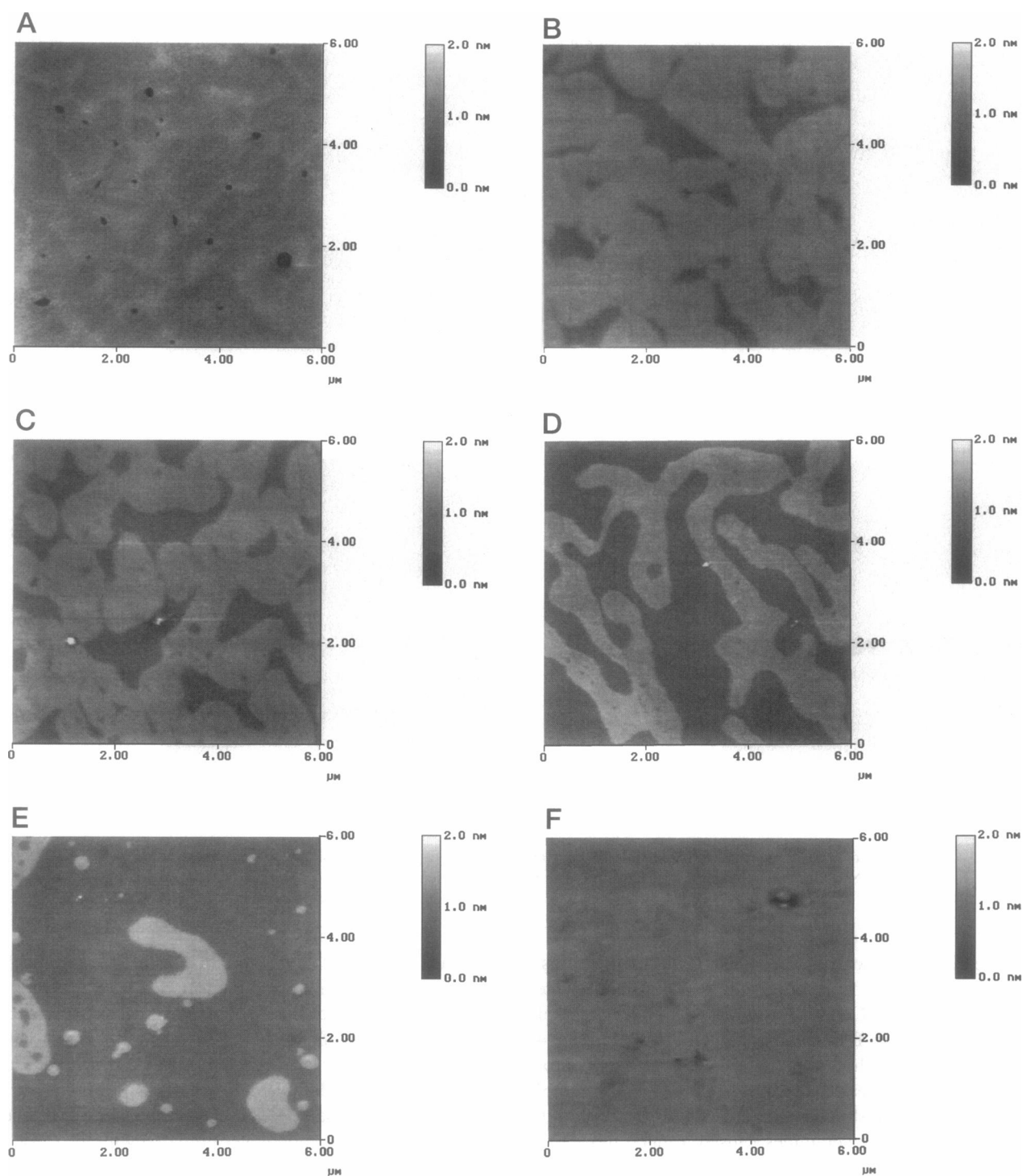


FIGURE 3 AFM images showing  $6 \mu\text{m} \times 6 \mu\text{m}$  areas of  $\Sigma\text{CerIII-Chol}$  mixed monolayers deposited upon silicon oxide substrates.  $\Sigma\text{CerIII-Chol}$  molar ratios are (a) 1:0, (b) 1:0.1, (c) 1:0.2, (d) 1:0.6, (e) 1:1, and (f) 1:2.

### Influence of addition of free fatty acids to pigskin ceramide-cholesterol mixtures

Free fatty acids of different chain lengths were added to a 1:1 mixture of pigskin ceramide-cholesterol to yield a 1:1:1 mixture. Fig. 5 A shows an AFM image of a monolayer prepared with a 1:1:1 mixture of pigskin ceramide-choles-

terol-palmitic acid (16:0). The shapes and sizes of the domains have changed compared with those of the 1:1 pigskin ceramide-cholesterol mixture (Fig. 2 B). The height difference between the two phases is  $13 \pm 1 \text{ \AA}$ . Only 31% of the surface is covered with the higher phase. Without fatty acids 40% of the surface is covered with the higher

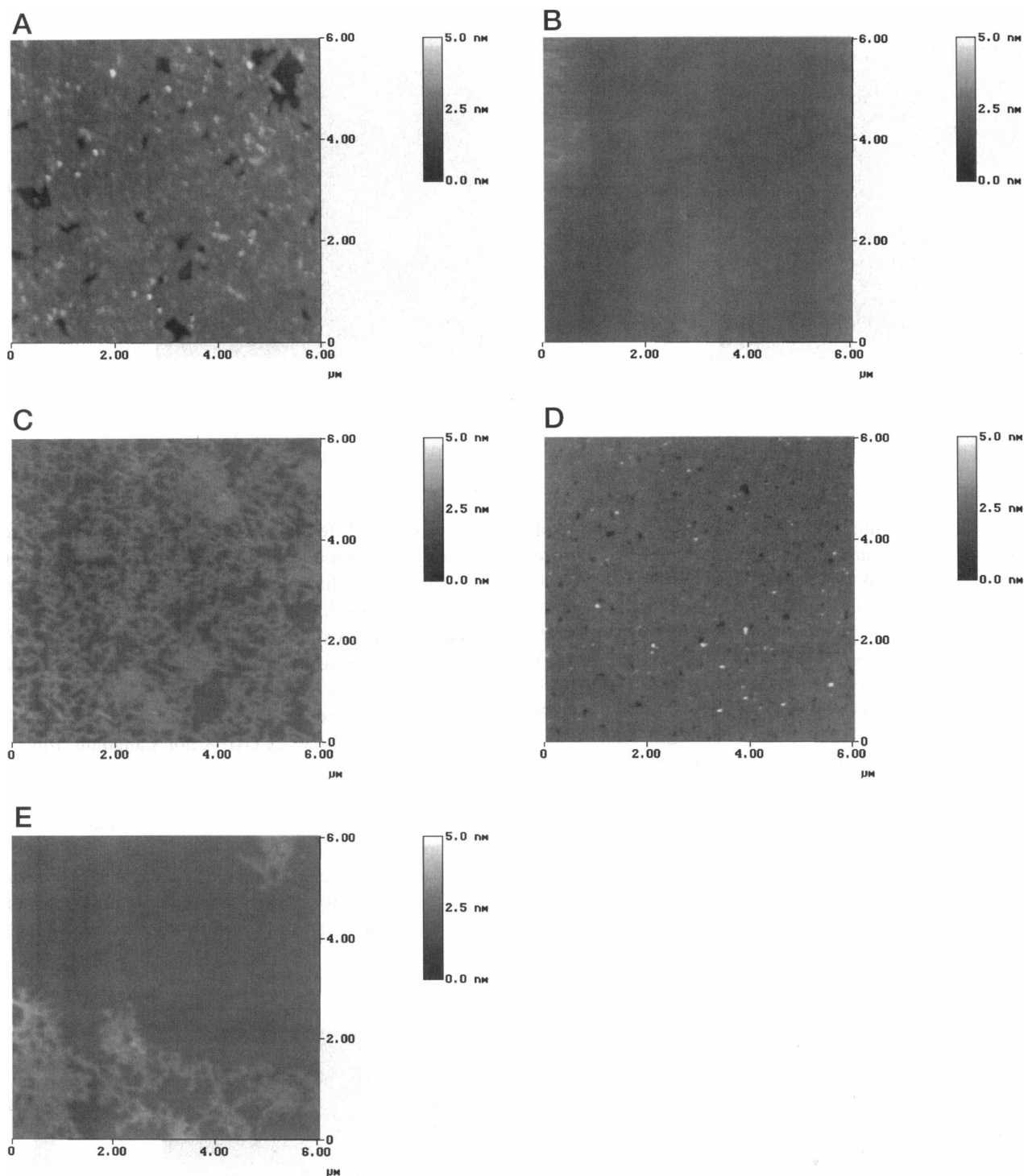


FIGURE 4 AFM images showing  $6\ \mu\text{m} \times 6\ \mu\text{m}$  areas of silicon oxide supported mixed monolayers of (a) C24cer3, (b) C16cer3:Chol 1:1, (c) C24cer3:Chol 1:1, (d) C16cer3:C24cer3 1:1, and (e) C16cer3:C24cer3:Chol 1:1:2.

phase. Fig. 5b shows an AFM image of a 1:1:1 pigskin ceramide-cholesterol-lignoceric acid (24:0) monolayer. The shapes of the domains are similar to those of the mixture with palmitic acid, but the fraction of the surface covered by the domains is larger (50%). The height difference between the domains and the surrounding molecules is  $16 \pm 1\ \text{\AA}$ .

#### Influence of addition of free fatty acids to $\Sigma\text{CerIII}$ -cholesterol mixtures

The influence of the addition of free fatty acids to a 1:1 mixture of  $\Sigma\text{CerIII}$ :Chol was also investigated. Adding palmitic acid (PA) did not change the morphology of the monolayer much. Fig. 6 A shows an AFM image of a 1:1:1



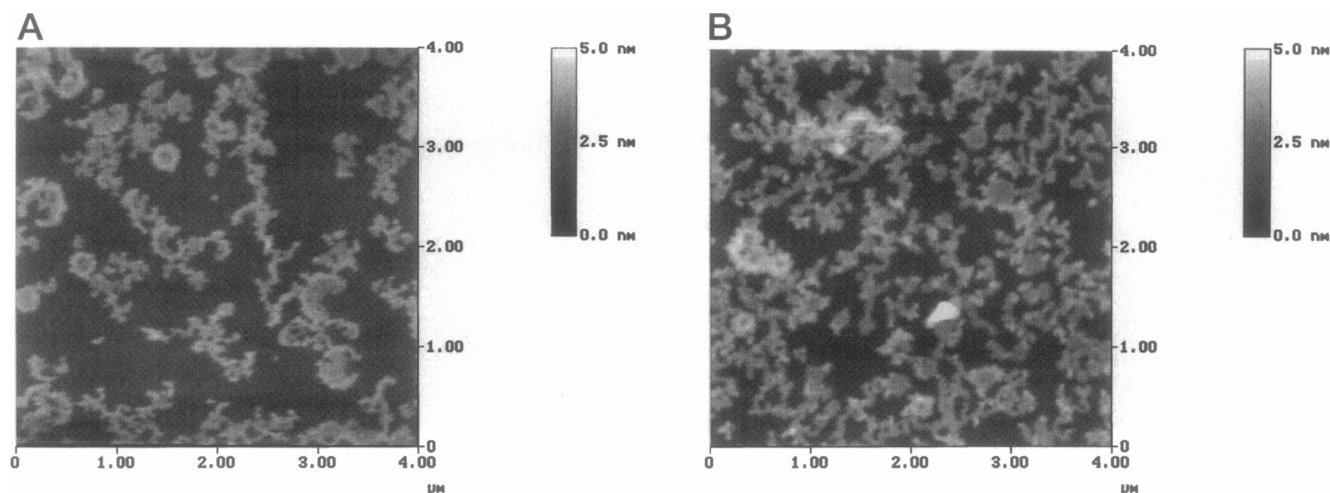


FIGURE 5 (A) AFM image of a  $4\ \mu\text{m} \times 4\ \mu\text{m}$  area of a mixed pigskin ceramide-Chol-PA acid 1:1:1 monolayer deposited upon a silicon oxide substrate. (B) AFM image of a  $4\ \mu\text{m} \times 4\ \mu\text{m}$  area of a mixed pigskin ceramide-Chol-LA 1:1:1 monolayer deposited upon a silicon oxide substrate.

$\Sigma$ CerIII-Chol-PA mixture. Some domain structures of phase A are visible, and also some very small features are visible within phase B that have a slightly larger height. The regular domains have a height of  $6 \pm 1\ \text{\AA}$ . When lignoceric acid (LA) was added, much smaller domains were formed. The AFM image in Fig. 6 B of a 1:1:1  $\Sigma$ CerIII-Chol-LA mixed monolayer shows many small, circular domains, which are interconnected. The difference in monolayer thickness between the two phases is larger than in the  $\Sigma$ CerIII-Chol mixed monolayer at a value of  $13 \pm 1\ \text{\AA}$ .

## DISCUSSION

### Mixtures of ceramides and cholesterol

We have shown here that AFM can be used to image phase separated monolayers composed of SC lipids. SC lipids

were mixed in different quantities to give a wide range of compositions. Monolayers were constructed by the Langmuir-Blodgett technique. A monolayer prepared with pure pigskin ceramide had an irregular surface with holes and ripples. This was expected on the basis of the rigidity of the film on the water-air interface. A monolayer prepared with a pigskin ceramide-cholesterol mixture had a fluidlike behavior. According to the surface pressure area isotherms the molecular area of the  $\Sigma$ CerIII-Chol Langmuir films followed the additivity rule (not shown). The fluidizing effect of cholesterol is attributed to an increased chain mobility toward the methyl end of the hydrophobic chains caused by the shape and height of the cholesterol molecule. Therefore the mean molecular area will not change. The fluidizing effects of cholesterol can be illustrated by the dissipation of a phase transition and the formation of an intermediate gel

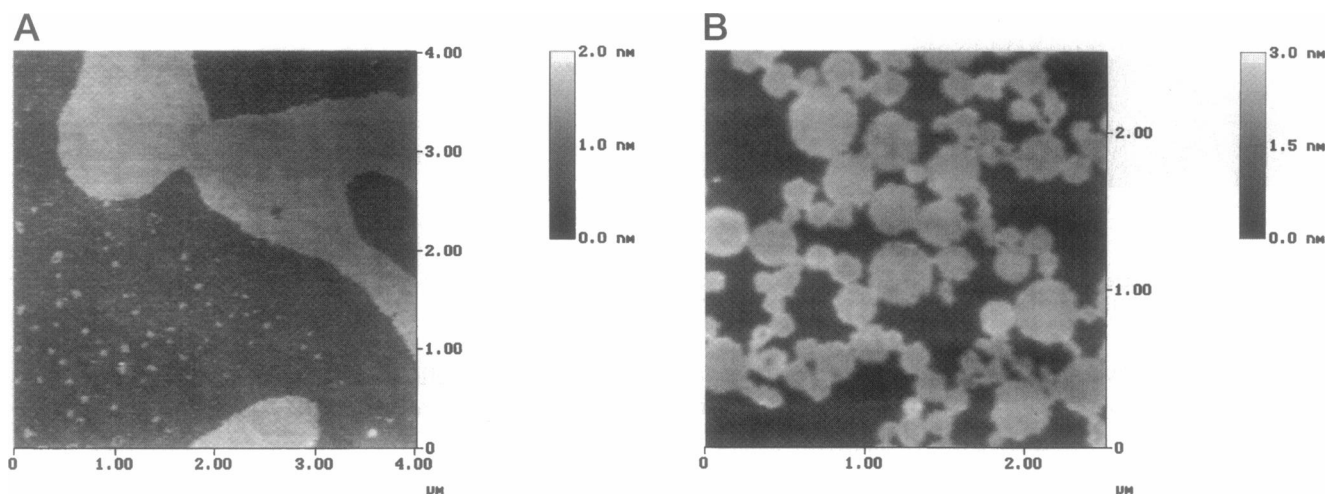


FIGURE 6 (A) AFM image of a  $4\ \mu\text{m} \times 4\ \mu\text{m}$  area of a mixed  $\Sigma$ CerIII-Chol-PA 1:1:1 monolayer deposited upon a silicon oxide substrate. (B) AFM image of a  $2.5\ \mu\text{m} \times 2.5\ \mu\text{m}$  area of a mixed  $\Sigma$ CerIII-Chol-LA acid 1:1:1 monolayer deposited upon a silicon oxide substrate.



state (Demel and de Kruijff, 1976). The AFM image showed that there were no holes in this film. However, it could be observed that two phases with a height difference of 8 Å were formed.

The phase behavior of the ceramides was investigated in more detail with  $\Sigma$ CerIII–cholesterol mixtures. After transfer of the monolayers to silicon oxide substrates the AFM images showed that mixed monolayers with  $\Sigma$ CerIII–Chol molar ratios between 1:0.1 and 1:1 consisted of two separate phases, which we call phase A and phase B. The fraction of the surface covered by phase A was measured by analysis of the AFM images. Fig. 7 shows the fraction of the surface covered by phase A as a function of the mole fraction of cholesterol. The characters marked a–f in the figure correspond to the AFM images in Fig. 3. Some of the data points in this figure correspond to mixtures of which we did not show the AFM images.

The fit drawn in Fig. 7 is a least-squares fit, which had only the compositions of phases A and B,  $x_A$  and  $x_B$ , as variables. The fraction  $F$  can be written as  $F = (N_A A_A) / (N_A A_A + N_B A_B)$ , with  $N_A$  and  $N_B$  the number of molecules and  $A_A$  and  $A_B$  the molecular surface areas of phases A and B, respectively. In the case of phase separation the lever rule is used:  $N_A(x_0 - x_A) = N_B(x_B - x_0)$ , where  $x_0$  is the initial composition expressed as the mole fraction of cholesterol. The molecular surface areas were assumed to follow the

additivity rule,  $A_A = x_A A_{\text{Chol}} + (1 - x_A) A_{\Sigma\text{CerIII}}$ , and  $A_B = x_B A_{\text{Chol}} + (1 - x_B) A_{\Sigma\text{CerIII}}$ . For  $A_{\text{Chol}}$  and  $A_{\Sigma\text{CerIII}}$  we used the values found from the  $\Pi$  A isotherms. Eventually, we found for the fraction  $F$

$$F = \frac{(x_B - x_0)(x_A A_{\text{Chol}} + (1 - x_A) A_{\Sigma\text{CerIII}})}{(x_B - x_0)(x_A A_{\text{Chol}} + (1 - x_A) A_{\Sigma\text{CerIII}}) + (x_0 - x_A)(x_B A_{\text{Chol}} + (1 - x_B) A_{\Sigma\text{CerIII}})}$$

The least-squares fit yielded the curve drawn in Fig. 7. For the composition of phases A and B we found  $x_A = 0$  and  $x_B = 0.56$ . This means that phase A is a pure  $\Sigma$ CerIII phase and that phase B is a mixed phase with a  $\Sigma$ CerIII–Chol molar ratio of approximately 1:1. We suggest that this is caused by the distribution of the fatty acid chain length in  $\Sigma$ CerIII. Our results can be explained if we assume that cholesterol mixes well with the short fatty acid chain  $\Sigma$ CerIII fraction and that cholesterol does not mix, or mixes to a lesser extent, with the long fatty acid chain  $\Sigma$ CerIII fraction. In that case, the phases observed in the AFM images of the phase separated monolayers were a pure  $\Sigma$ CerIII phase (A), containing (18:0) and mainly (24:1)  $\Sigma$ CerIII, and a mixed equimolar (18:0)  $\Sigma$ CerIII–cholesterol phase (B). This is also in agreement with the differences in monolayer thickness of  $\sim 5$  Å that we found in the  $\Sigma$ CerIII–Chol mixed monolayers. The expected difference in thickness is somewhat greater because the difference in fatty acid chain length is 6 C atoms, but that can be explained by the depression of the monolayer by the AFM tip (Wolthaus et al., 1994). At cholesterol concentrations higher than 1:1 the interaction between cholesterol and the long-chain  $\Sigma$ CerIII fraction has become high enough to incorporate the long-chain  $\Sigma$ CerIII fraction into the mixed short-chain  $\Sigma$ CerIII fraction–cholesterol phase, resulting in one homogeneous phase.

We investigated the hypothesis that cholesterol mixed primarily with short fatty acid chain  $\Sigma$ CerIII by preparing mixed monolayers composed of one or both of the two synthetic ceramides, cholesterol, or both. We observed that in the C16cer3–Chol 1:1 mixed monolayer phase separation did not occur and that in this case ideal mixing behavior was observed. Contrary to that, the C24cer3–Chol 1:1 mixture showed domain structures, which were most likely caused by separation of the mixture in a C24cer3 fraction and a cholesterol fraction. The difference in monolayer thickness between the domains and the surrounding molecules is  $\sim 6$  Å, which is slightly larger than the difference in monolayer thickness in the phase separated  $\Sigma$ CerIII–Chol mixed monolayers. This is not surprising, because in the C24cer3–Chol monolayers the two phases consist of (24:0) ceramide3 and cholesterol, respectively, whereas in the  $\Sigma$ CerIII–Chol system we measured the difference in monolayer thickness between (24:1)  $\Sigma$ CerIII and the phase containing cholesterol and (18:0)  $\Sigma$ CerIII. A mixture of C16cer3 and C24cer3 did not phase separate. This is in good agreement with the behavior of the pure  $\Sigma$ CerIII monolayer, where we also observed a homogeneous film. When we added cholesterol

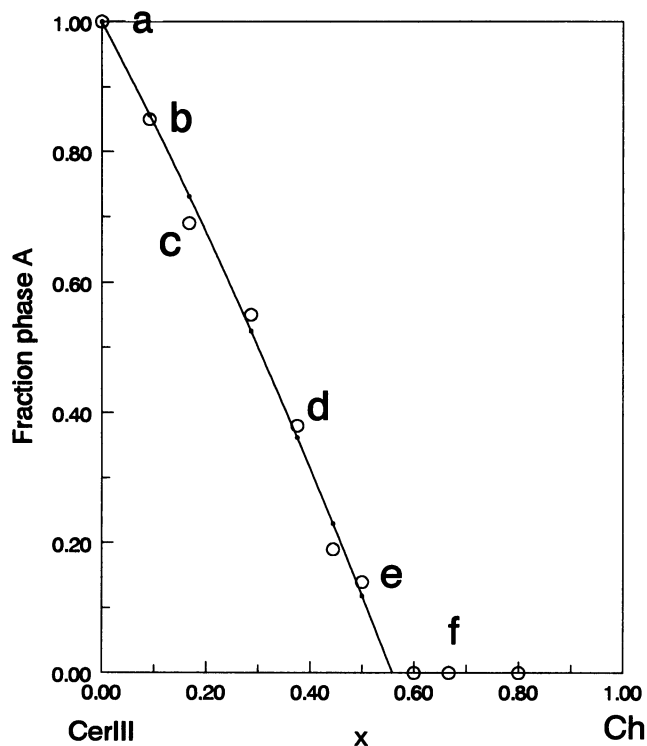


FIGURE 7 Graph showing the fraction of the surface covered by phase A as a function of the mole fraction of cholesterol in  $\Sigma$ CerIII–Chol mixed monolayers. Characters in the graph correspond to the AFM images shown in Fig. 2. The line is a least-squares fit of the phase separation model discussed in the text.

to a 1:1 mixture of C16cer3 and C24cer3 we found domains that were similar to the domains found in the C24cer3-Chol monolayers. This is a strong indication that the domain structures originate from the long fatty acid chain ceramide molecules and that the other phase contains cholesterol and the short fatty acid chain ceramide. The shapes of the domains were not similar to those of the domains in the  $\Sigma$ CerIII-Chol mixed monolayers, although the total composition of the ceramides in this mixture resembled the  $\Sigma$ CerIII composition to a large extent. Obviously, there were still too many differences between this mixture and  $\Sigma$ CerIII. The most significant difference we noticed is that part of the  $\Sigma$ CerIII molecules have long monounsaturated fatty acid chains, whereas the synthetic ceramide molecules all have saturated fatty acid chains. This could cause a different packing of the molecules and as a result of that a difference in the domain shapes.

### Mixtures of ceramides, cholesterol, and free fatty acids

The addition of free fatty acids to a ceramide-cholesterol mixture led to different structures for PA (16:0) and LA (24:0). The mixed monolayers prepared with Tcer-Chol and PA or LA had the same structure, which was different from that of the Tcer-Chol monolayer. However, the fraction of the surface covered with domains was lower than in the Tcer-Chol monolayer if PA was added and higher if LA was added. Therefore, it seems reasonable to assume that PA mixes with the short fatty acid chain fraction of Tcer and with cholesterol and that LA mixes with the long fatty acid chain fraction of Tcer.

Monolayers prepared with  $\Sigma$ CerIII-Chol and PA or LA showed a slightly different behavior. A mixed monolayer prepared with  $\Sigma$ CerIII-Chol-PA with a 1:1:1 molar ratio had a structure similar to that of a  $\Sigma$ CerIII-Chol monolayer, which also had large domains with curved edges. The difference in monolayer thickness between the two phases was 6 Å, which is in good agreement with the difference in monolayer thickness found in  $\Sigma$ CerIII-Chol monolayers. If we added LA instead of PA we found a structure that consisted of small round domains, which covered ~50% of the surface. The domains were 13 Å higher than the rest of the surface. We believe that the difference in the structures of the monolayers prepared with PA and those prepared with LA can be explained by the difference in fatty acid chain length of the acids. PA will most likely mix with the short fatty acid chain  $\Sigma$ CerIII fraction and with cholesterol, which are both dominantly present in phase B, which has the smallest thickness. PA does not mix with the long fatty acid chain fraction of  $\Sigma$ CerIII. Phase A, the phase that forms the domain structures, still consists only of (24:1)  $\Sigma$ CerIII molecules, and therefore the domain shape and also the difference in monolayer thickness between phases A and B will be similar to the thickness found in  $\Sigma$ CerIII-Chol monolayers. On the other hand, LA will most likely mix

with the long fatty acid chain  $\Sigma$ CerIII fraction. LA is then incorporated into the domains and forms one phase with the (24:1)  $\Sigma$ CerIII molecules. This explains the large fraction of the surface covered by the domains. Another effect is that it causes a change in the domain shape and probably also in the molecular structures of the domains. The fatty acid chains of the molecules in the domains are more densely packed, and therefore the domains are more rigid than without LA. As a result of this the domains are not depressed as much as before by the AFM tip, whereas the structure of the cholesterol-rich phase is the same as in the  $\Sigma$ CerIII-Chol monolayer. This could be the reason for the larger difference in monolayer thickness that we measured with this monolayer.

### Comparison with the formation of lamellar phases in bulk mixtures

Recently the lipid organization in the SC and in mixtures of ceramides and cholesterol were studied by x-ray diffraction. From these studies it could be concluded that the lipids in the SC are organized in two lamellar phases with repeat distances of approximately 6 and 13 nm, respectively. Recently these phases were also found in mixtures of  $\Sigma$ CerIII and cholesterol (Parrott and Turner, 1993) and isolated pig ceramides and cholesterol (Bouwstra et al., submitted) over a wide composition range. These compositions range for the mixture of  $\Sigma$ CerIII and cholesterol from 1:0.2 to 1:1 and for the mixture of Tcer and cholesterol from 1:0.2 to 1:2, respectively.

Although the monolayer approach cannot mimic the phase behavior in bulk mixtures prepared from cholesterol and ceramides because the 13-nm phase consists of more than one bilayer in the unit cell and the ceramides are very asymmetric in chain length, we can draw important conclusions for the formation of the 6- and 13-nm lamellar phases from the results described in this paper. With respect to the conclusions, two observations are very important, namely, 1) for phase separation in the monolayer a bimodal distribution of the chain lengths of the ceramides is required; the "long-chain ceramides" and "short-chain ceramides" do not mix at moderate cholesterol contents; and 2) the two phases found in the monolayer approach and in the bulk mixtures (as measured by x-ray diffraction) occur in approximately the same ceramide-cholesterol concentration range. The latter observation strongly indicates that the phase separations in the bulk mixture and in the monolayer are correlated, which led us to conclude that for the formation of the lamellar phases in the bulk mixtures a bimodal fatty acid chain length distribution in the ceramides is a prerequisite. It is most likely that in the bulk mixtures the "short-chain ceramides" and that the "long-chain ceramides" do not mix in the bilayers but form separate sublattices.

## REFERENCES

- Bouwstra, J. A., G. S. Gooris, J. A. van der Spek, and W. Bras. 1991. The structure of human stratum corneum as determined by small angle x-ray scattering. *J. Invest. Dermatol.* 96:1005–1012.
- Bouwstra, J. A., G. S. Gooris, J. A. van der Spek, S. Lavrijsen, and W. Bras. 1994. The lipid and protein structure of mouse stratum corneum: a wide and small angle diffraction study. *Biochim. Biophys. Acta.* 1212:183–192.
- Bouwstra, J. A., G. S. Gooris, W. Bras, and D. T. Downing. 1995. The lipid and keratin structure of pig stratum corneum. *J. Lipid Res.* 36:685–695.
- Bouwstra, J. A., G. S. Gooris, K. Cheng, A. Weerheim, W. Bras, and M. Ponc. 1996. Isolated stratum corneum lipids as a model for the skin barrier. *J. Lipid Res.* 37:999–1011.
- Breathnach, A. S., T. Goodman, C. Stolinky, and M. Gross. 1973. Freeze-fracture replication of cells of stratum corneum of human epidermis. *J. Anat.* 114:65–81.
- Elias, P. M. 1983. Epidermal lipids, barrier function, and desquamation. *J. Invest. Dermatol.* 80:44s–49s.
- Demel, R. A., and B. de Kruijff. 1976. The function of sterols in membranes (review). *Biochim. Biophys. Acta.* 457:109–132.
- Fujihira, M., and H. Tanako. 1994. Observation of the phase-separated Langmuir–Blodgett films on vapor-deposited silver films with atomic force microscopy and friction force microscopy. *Thin Solid Films.* 243:446–449.
- Ge, S., A. Takahara, and T. Kajiyama. 1995. Phase separated morphology of an immobilized organosilane monolayer studied by a scanning probe microscope. *Langmuir.* 11:1341–1346.
- Löfgren, H., and I. Pascher. 1977. Molecular arrangements of spingolipids. The monolayer behavior of ceramides. *Chem. Phys. Lipids.* 20:273–284.
- Meyer, E., R. Overney, R. Lüthi, D. Brodbeck, L. Howald, J. Frommer, H.-J. Güntherodt, O. Wolter, M. Fujihira, H. Tanako, and Y. Gotoh. 1992. Friction force microscopy of mixed Langmuir–Blodgett films. *Thin Solid Films.* 220:132–137.
- Overney, R. M., E. Meyer, J. Frommer, D. Brodbeck, R. Lüthi, L. Howald, H.-J. Güntherodt, M. Fujihira, H. Takano, and Y. Gotoh. 1992. Friction measurements on phase-separated thin films with a modified atomic force microscope. *Nature (Lond.).* 359:133–135.
- Overney, R. M., T. Bonner, E. Meyer, M. Rüetschi, R. Lüthi, L. Howald, J. Frommer, H.-J. Güntherodt, M. Fujihira, and H. Takano. 1994. Elasticity, wear, and friction properties of thin organic films observed with atomic force microscopy. *J. Vac. Sci. Technol. B.* 12:1973–1976.
- Parrott, D. E., and J. E. Turner. 1993. Mesophase formation by ceramides and cholesterol. *Biochim. Biophys. Acta.* 1147:273–276.
- Schurer, N. Y., and P. M. Elias. 1991. The biochemistry and function of stratum corneum lipids. In *Skin Lipids*. P. M. Elias, editor. Academic Press, Advances in Lipid Research, 24:27–56.
- Wertz, P. W., and D. T. Downing. 1983. Ceramides of pid epidermis: structure determination. *J. Lipid Res.* 24:759–765.
- Wertz, P. W., and D. T. Downing. 1991. Epidermal lipids. In *Physiology, Biochemistry, and Molecular Biology of the Skin*. L. A. Goldsmith, editor. Oxford University Press, New York. 205–236.
- White, S. H., D. Mirejovsky, and G. I. King. 1988. Structure of lamellar lipid domains and corneocyte envelopes of murine stratum corneum. An x-ray diffraction study. *Biochemistry.* 27:3725–3732.
- Wolthaus, L., A. Schaper, and D. Möbius. 1994. Microcrystallinity of solid-state Langmuir–Blodgett films of saturated fatty acids studied by scanning force microscopy and brewster angle microscopy. *J. Phys. Chem.* 98:10,809–10,813.
- Wu, H.-M., S.-J. Xiao, Z.-H. Tai, and Y. Wei. 1995. Polymorphism of domains in phase-separated Langmuir–Blodgett films. *Phys. Lett. A.* 199:119–122.
- Xiao, S.-J., H.-M. Wu, X.-M. Yang, N.-H. Li, Y. Wei, X.-Z. Sun, and Z.-H. Tai. 1995. Morphologies of phase-separated monolayers investigated by atomic force microscopy. *Thin Solid Films.* 256:210–214.
- Yang, X.-M., S.-J. Xiao, Z.-H. Lu and Y. Wei. 1994. Observation of phase separation of phospholipids in mixed monolayer Langmuir–Blodgett films by atomic force microscopy. *Surf. Sci.* 316:L1110–L1114.